Atmospheric Environment 140 (2016) 539–554

Contents lists available at ScienceDirect

Atmospheric Environment

journal homepage: www.elsevier.com/locate/atmosenv

Contribution of regional-scale fire events to ozone and $PM_{2.5}$ air quality estimated by photochemical modeling approaches

K.R. Baker [a, *], M.C. Woody [b], G.S. Tonnesen [c], W. Hutzell [b], H.O.T. Pye [b], M.R. Beaver [a], G. Pouliot [b], T. Pierce [b]

[a] U.S. Environmental Protection Agency, Office of Air Quality Planning and Standards, 109 TW Alexander Dr., Research Triangle Park, NC 27711, United States
[b] U.S. Environmental Protection Agency, Office of Research and Development, 109 TW Alexander Dr., Research Triangle Park, NC 27711, United States
[c] U.S. Environmental Protection Agency, Region 8, 1595 Wynkoop Street, Denver, CO 80202, United States

HIGHLIGHTS

- Photochemical model source apportionment can track fire impacts on O_3 & PM.
- Light attenuating properties of PM have notable impacts on fire O_3 estimates.
- Modeled organic aerosol from fire varies using traditional & VBS approaches.
- Model often overestimates O_3 when model predicts high fire impact.
- Emissions and chemical production contribute to modeled HCHO in excess of 25 ppb.

ARTICLE INFO

Article history:
Received 26 February 2016
Received in revised form
10 June 2016
Accepted 14 June 2016
Available online 15 June 2016

Keywords:
Wild fire
Prescribed fire
Photochemical model
Ozone
Particulate matter

ABSTRACT

Two specific fires from 2011 are tracked for local to regional scale contribution to ozone (O_3) and fine particulate matter ($PM_{2.5}$) using a freely available regulatory modeling system that includes the BlueSky wildland fire emissions tool, Spare Matrix Operator Kernel Emissions (SMOKE) model, Weather and Research Forecasting (WRF) meteorological model, and Community Multiscale Air Quality (CMAQ) photochemical grid model. The modeling system was applied to track the contribution from a wildfire (Wallow) and prescribed fire (Flint Hills) using both source sensitivity and source apportionment approaches. The model estimated fire contribution to primary and secondary pollutants are comparable using source sensitivity (brute-force zero out) and source apportionment (Integrated Source Apportionment Method) approaches. Model estimated O_3 enhancement relative to CO is similar to values reported in literature indicating the modeling system captures the range of O_3 inhibition possible near fires and O_3 production both near the fire and downwind. O_3 and peroxyacetyl nitrate (PAN) are formed in the fire plume and transported downwind along with highly reactive VOC species such as formaldehyde and acetaldehyde that are both emitted by the fire and rapidly produced in the fire plume by VOC oxidation reactions. PAN and aldehydes contribute to continued downwind O_3 production. The transport and thermal decomposition of PAN to nitrogen oxides (NO_X) enables O_3 production in areas limited by NO_X availability and the photolysis of aldehydes to produce free radicals (HO_X) causes increased O_3 production in NO_X rich areas. The modeling system tends to overestimate hourly surface O_3 at routine rural monitors in close proximity to the fires when the model predicts elevated fire impacts on O_3 and Hazard Mapping System (HMS) data indicates possible fire impact. A sensitivity simulation in which solar radiation and photolysis rates were more aggressively attenuated by aerosol in the plume reduced model O_3 but does not eliminate this bias. A comparison of model predicted daily average speciated $PM_{2.5}$ at surface rural routine network sites when the model predicts fire impacts from either of these fires shows a tendency toward overestimation of $PM_{2.5}$ organic aerosol in close proximity to these fires. The standard version of the CMAQ treats primarily emitted organic aerosol as non-volatile. An alternative approach for treating organic aerosol as semi-volatile resulted in lower $PM_{2.5}$ organic aerosol from these fires but does not eliminate the bias. Future work should focus on modeling specific fire events that are well characterized in terms of size, emissions, and have extensive measurements taken near the fire and downwind

* Corresponding author.
E-mail address: baker.kirk@epa.gov (K.R. Baker).

http://dx.doi.org/10.1016/j.atmosenv.2016.06.032
1352-2310/Published by Elsevier Ltd.

to better constrain model representation of important physical and chemical processes (e.g. aerosol photolysis attenuation and organic aerosol treatment) related to wild and prescribed fires.

Published by Elsevier Ltd.

1. Introduction

Over the past 30 years, an average of 5 million acres of wildlands have burned annually, and this average has doubled in recent years (National Interagency Fire Center, 2016). Fires produce smoke plumes that impact air quality locally, regionally, and globally. Resulting ambient air pollutants with known deleterious human health impacts include particulate matter less than 2.5 μm in diameter ($PM_{2.5}$), ozone (O_3), and numerous air toxics (e.g. formaldehyde). These pollutants can cause cardiopulmonary health impacts (Diaz, 2015; Kim et al., 2014) leading to increased hospital admissions for asthma and increased rate of heart failure in exposed populations (Rappold et al., 2011). Wildland fires emit precursors including nitrogen oxides (NO_X) and volatile organic compounds (VOCs) that can react to form O_3 within the fire plume (Wiedinmyer et al., 2011), although in some situations, especially near the fire, O_3 formation may be inhibited or muted due to O_3 titration by fresh emissions of nitric oxide (NO) and reductions in solar radiation needed to drive photochemical reactions (Jiang et al., 2012). Fires also directly emit particles and precursors such as NO_X, sulfur dioxide (SO_2), ammonia (NH_3), and VOCs that can react in the plume and with the surrounding atmosphere to form secondary $PM_{2.5}$.

Many areas in the U.S. exceed levels of the O_3 and $PM_{2.5}$ National Ambient Air Quality Standards (NAAQS) and mandatory Class I areas (e.g. most National Parks and some wilderness areas) experience impaired visibility. It is important to determine the contribution from wildland fires to O_3 and $PM_{2.5}$ to develop effective strategies to meet the level of the NAAQS, to achieve regional haze goals, and for other purposes such as supporting an exceptional events demonstration which allows states to exclude ambient data from NAAQS design value calculation and potentially avoid a non-attainment designation for O_3 or PM. In addition, fires emit a variety of climate forcers (e.g., carbon dioxide (CO_2), black carbon, brown carbon) and these emissions may be increasing as fires increase in frequency and severity into the future (Keywood et al., 2013). The magnitude and ratios of emissions of various pollutants from wildland fires vary greatly depending on fire size, fuel characteristics, combustion efficiency, and meteorological conditions (Akagi et al., 2012). As a result of variable emissions, radiative impacts, and non-linear O_3 and $PM_{2.5}$ production chemistry, primary and secondary pollutants from fires are difficult to predict (Jaffe and Wigder, 2012). Several ambient measurement based studies have found enhancements in O_3 attributable to wildfire impacts (Bytnerowicz et al., 2013; Jaffe et al., 2013; Pfister et al., 2008). The contribution from wildland fires to $PM_{2.5}$ has been quantified to some degree by observed enhancement ratios and statistical models with varying levels of success (Forrister et al., 2015; May et al., 2015; Vakkari et al., 2014).

Photochemical grid models are used to make regulatory and scientific conclusions about fire impacts on both primary and secondary pollutants at local to continental scales. These models have been used to track the contribution from all wildland fires to O_3 and $PM_{2.5}$ (Fann et al., 2013) but rarely used for the contribution of specific fire events to both O_3 and $PM_{2.5}$. Chemical transport models have been applied to estimate the contribution of specific fire events to O_3 using a trajectory box model (Real et al., 2007) and photochemical transport model (Cai et al., 2016; McKeen et al., 2002). Photochemical transport models have also been used to estimate secondary $PM_{2.5}$ impacts from specific fires (Garcia-Menendez et al., 2013, 2014; Konovalov et al., 2015; Saide et al., 2015).

Modeling specific fire events allows for a clearer connection between emissions estimates and downwind impacts. Here, we applied a photochemical grid model for two large well known fire events from 2011 and differentiated the downwind impacts of these fires from other sources of pollution. Impacts are assessed for a wildfire (Wallow in eastern Arizona) and a prescribed fire (Flint Hills region of central and eastern Kansas). Both fires are tracked for contribution to O_3 and $PM_{2.5}$ using source sensitivity (brute-force zero out) and source apportionment methods. Source apportionment is often desirable in regulatory model applications where a contribution estimate is needed from specific sources or source complexes to the resulting air pollution at a given place and time (similar to ambient based apportionment approaches such as Positive Matrix Factorization or Chemical Mass Balance) rather than understanding how the atmosphere would change in the absence of a particular source (Kwok et al., 2015). The estimated impacts from these fires are constrained by comparing enhancement ratios for O_3 against those reported in literature and also against rural surface monitors measuring O_3 and chemically speciated $PM_{2.5}$ that are less influenced by other (e.g. urban) emissions sources.

Here, known large uncertainties in fire predicted secondary pollutant impacts are explored with sensitivity simulations where the model predicted organic carbon is more aggressively parameterized to attenuate photolysis rates and also treating organic aerosol (OA) as semi-volatile. Other studies applying photochemical transport models for fire impacts indicate that the attenuation of photolysis by aerosol from the fire has notable impacts on model predicted O_3 (Jiang et al., 2012) and the treatment of aerosol volatility can result in large changes in model estimated $PM_{2.5}$ from fires (Konovalov et al., 2015; May et al., 2013). Changes in surface O_3 from fire impacts on mixing layer height, temperature, and biogenic emission rates were minimal compared to photolysis impacts (Jiang et al., 2012). Some portion of primarily emitted $PM_{2.5}$ organic carbon may be semi-volatile and thus change the near-field and long-range form of OA impacts from fires (Jimenez et al., 2009; May et al., 2013). Therefore, both a traditional approach (non-volatile primary OA) and volatility basis set (VBS) approach that allows for semi-volatile primary OA and multigenerational aging of secondary organic aerosol (SOA) systems (Koo et al., 2014) were used to assess $PM_{2.5}$ impacts from these fires. The CMAQ-VBS approach has been compared with the standard version of CMAQ and with field study measurements in an urban area (Woody et al., 2016) but little evaluation is available for areas heavily influenced by biomass burning (Konovalov et al., 2015).

2. Methods

An integrated modeling system used to support U. S. Environmental Protection Agency rules and air quality standards development was used for estimating primary and secondary pollutant impacts from specific fire events. The Weather Research and Forecasting (WRF) model was applied to generate the necessary

meteorological data that is used as input to the Sparse Matrix Operator Kernel Emissions (SMOKE) model and the Community Multiscale Air Quality (CMAQ) three-dimensional Eulerian photochemical transport model. Further, the SMOKE model used wildland fire emissions generated using the Satellite Mapping Automated Reanalysis Tool for Fire Incident Reconciliation (SmartFire) – BlueSky framework as provided by the U.S. Forest Service (Raffuse et al., 2012). All of these models are well documented, freely available to the modeling community, and have been extensively used to support both regulatory and scientific air quality assessments.

Two different large and generally well characterized fires from 2011 are tracked for contribution. These fires were selected to represent different seasons, biomass fuel types, and geographic area of the country. The Wallow fire consumed over 2180 square km of alpine conifer biomass between May 29 and July 8 during 2011 in eastern Arizona and western New Mexico (U.S. Department of Agriculture, 2011). The Wallow fire is currently the largest fire on record for Arizona. Prescribed fires are often set in the tall grass prairie Flint Hills region of eastern Kansas for land management purposes and can exceed 8000 to 12,000 square km. These prescribed fires are typically set in April, but in periods of extreme drought little or no fires may be set so not every year has a large scale prescribed burn (Kansas Department of Health and Environment, 2010).

CMAQ version 5.0.2 was applied to simulate portions of two different fire events in 2011 (Figure S1): Wallow (June 1 to June 6) and Flint Hills (April 1 to April 15). Initial conditions were extracted from an annual 2011 CMAQ simulation using the same domain specifications. Meteorological input was generated using version 3.4.1 of the WRF prognostic meteorological model (Skamarock et al., 2008). Both modeling systems were applied using the same grid projection and model domain covering the continental United States with 12 square km sized grid cells (Figure S1). Additional details about WRF configuration and evaluation are provided elsewhere (U.S. Environmental Protection Agency, 2014b). The atmosphere up to 50 mbars (mb) was resolved with 25 layers in CMAQ and 35 layers in WRF. Layers are thinnest in the boundary layer to better capture the diurnal variation in boundary layer height. Chemical boundary inflow was extracted from a global model simulation for 2011 and varies in space and time (Henderson et al., 2014).

2.1. Emissions

Anthropogenic emissions were based on version 2 of the 2011 National Emission Inventory (NEI) (U.S. Environmental Protection Agency, 2014a). Temperature and solar radiation from WRF were used to generate hourly biogenic emissions with the BEIS version 3.61 model (Bash et al., 2016; Carlton and Baker, 2011). Emissions were speciated, spatially allocated to the grid, and temporalized using version 3.6.5 of the SMOKE emissions model (Houyoux et al., 2000). Primary emitted mass associated with carbon (NCOM) was based on OM:OC ratios that vary by emissions source sector (Simon and Bhave, 2012).

Wildfire and prescribed fire emissions, collectively called wildland fires, were included when and where these emissions occur within the model domain. These day specific emissions were based on the latest version of the SmartFire version 2 (Raffuse et al., 2012) and the BlueSky emissions framework. Detailed information about how the EPA develops wildland fire inventories can be found in the 2011 NEI Technical Support Document (U.S. Environmental Protection Agency, 2014a). Currently, the inventory distinguishes between prescribed, wild, and agricultural fire types based on satellite detection information. The BlueSky fire emissions modeling framework used here includes Fuels Characterization Classification System (FCCS) version 2 fuel loading model, CONSUME version 5 fuel consumption model, and Fire Emission Production Simulator (FEPS) version 2 emission factors. Fire location based satellite detection (SmartFire) or on-the-ground information is provided to FCCS to determine the fuel type, which is input to CONSUME along with an estimate of the area burned from SmartFire. The CONSUME model estimates the amount of fuel burned and the flaming and smoldering fraction which is used by FEPS to estimate daily emissions of CO, NO_X, VOC, and primarily emitted $PM_{2.5}$.

The FEPS estimated emissions are translated to chemical mechanism specific emissions by the SMOKE model using speciation factors. NO_X emissions were speciated as 90% NO and 10% NO_2. A single speciation profile (SPECIATE database profile 5560) was used to map all wildland fire emissions of total organic gases (TOG) to specific compounds matching the Carbon-Bond gas phase chemistry lumping scheme (Table 1). Approximately 40% of TOG emissions were speciated to unreactive and very slowly reactive (e.g., methane) compounds. Similarly, a single profile (SPECIATE database profile 91,102) was used to map total $PM_{2.5}$ emissions from fires to specific compounds (Table 1). The $PM_{2.5}$ speciation profile is largely organic aerosol (78%) and elemental carbon (9%) which is fairly similar to the composition measured near a savannah fire event (Vakkari et al., 2014), sagebrush (Pratt et al., 2011), grasses, and forest (Strand et al., 2015). The fraction of organic mass (OM) to organic carbon is 1.7 (Simon and Bhave, 2012) for wild and prescribed fires. Primarily emitted carbon (organic and elemental) were assumed to be 99.9% in the accumulation mode and 0.1% in the Aitken mode (Nolte et al., 2015). Wild and prescribed fire daily emissions were largely temporally allocated to daytime hours and this is most pronounced with prescribed fires that have a sharp increase in the early morning and decrease in the early evening (Figure S2) which is related to fire management practices.

Plume rise from fires is calculated using the Pouliot-Godowitch algorithm that converts BlueSky provided fire-specific information (e.g. area burned, fuel loading, heat content, and duration) to daily heat and buoyancy flux. The top and bottom of the plume is estimated using the Briggs plume rise approach (Paugam et al., 2015). A smoldering fraction of total fire emissions is estimated based on the buoyant efficiency which is a function of area burned. The smoldering emissions are evenly distributed vertically from the surface

Table 1
$PM_{2.5}$ and total organic gas (TOG) speciation profiles for wild and prescribed fires used as part of this modeling assessment. TOG species names correspond to the CB05 mechanism.

$PM_{2.5}$ specie	Fraction	TOG specie	Fraction
POC	0.46180	UNR	0.219
PNCOM	0.32320	PAR	0.184
PEC	0.09490	CH4	0.178
PCL	0.04150	FORM	0.084
PK	0.02940	MEOH	0.076
PMOTHR	0.01370	OLE	0.069
PSO4	0.01260	ALD2	0.054
PNH4	0.00879	ETH	0.042
PNA	0.00573	TOL	0.025
PCA	0.00386	ALDX	0.024
PSI	0.00182	ETHA	0.023
PNO3	0.00132	BENZENE	0.019
PAL	0.00061	TERP	0.008
PFE	0.00043	XYL	0.006
PMG	0.00031	IOLE	0.005
PTI	0.00005	ISOP	0.004
PMN	0.00002	ETOH	0.001

Table 2
Daily emissions (tons per day) for the Wallow and Flint Hills fires. PEC = $PM_{2.5}$ elemental carbon; POA = $PM_{2.5}$ organic aerosol; OTHPM = Total primarily emitted $PM_{2.5}$ excluding both PEC and POA.

Event	MMDD	CO	VOC	NO_X	POA	PEC	OTHPM	SO_2	NH_3
Flint hills	01/04/2011	29,269	7025	827	2429	311	107	351	489
	02/04/2011	50,828	12,188	1395	4192	537	184	596	848
	03/04/2011	15,870	3801	421	1299	166	57	182	264
	04/04/2011	4305	1033	120	357	46	16	51	72
	05/04/2011	19,307	4632	539	1598	205	70	229	322
	07/04/2011	12,131	2908	331	999	128	44	142	202
	08/04/2011	57,315	13,734	1538	4704	603	207	662	955
	09/04/2011	60,614	14,534	1664	4999	640	220	711	1011
	10/04/2011	10,622	2548	296	879	113	39	126	177
	11/04/2011	55,738	13,355	1494	4574	586	201	643	929
	12/04/2011	1,03,900	24,927	2900	8600	1102	378	1234	1734
	13/04/2011	61,662	14,789	1703	5092	652	224	727	1029
	14/04/2011	10,144	2432	278	836	107	37	119	169
	15/04/2011	352	85	10	29	4	1	4	6
Wallow	01/06/2011	4002	948	67	278	34	43	34	66
	02/06/2011	53,554	12,621	681	3595	435	550	387	878
	03/06/2011	41,547	9799	554	2804	339	429	308	682
	04/06/2011	84,893	20,020	1126	5726	692	876	628	1393
	05/06/2011	71,742	16,924	970	4850	586	742	536	1177
	06/06/2011	92,120	21,729	1239	6224	752	952	687	1512

to plume bottom. Non-smoldering emissions are evenly distributed vertically between the plume bottom and top (U.S. Environmental Protection Agency, 2015). Both smoldering and non-smoldering components of the fire have the same emissions composition.

2.2. Photochemical model

The CMAQ model was applied using ISORROPIA II inorganic aerosol partitioning (Fountoukis and Nenes, 2007), CB05TU gas-phase chemistry with updated toluene reactions (Sarwar et al., 2011), and aqueous phase chemistry that includes sulfur oxidation (Sarwar et al., 2013). The CMAQ v5.0.2 standard organic aerosol treatment (called AE6) includes nonvolatile primarily emitted organic aerosol (POA) and secondarily formed organic aerosol (SOA) from oxidation of traditional VOC precursors (toluene, xylenes, benzene, isoprene, monoterpenes, and sesquiterpenes) and SOA formed in clouds. CMAQ also includes an alternative approach to treat organic aerosol with the volatility basis set (Koo et al., 2014) that includes multigenerational oxidation of traditional SOA systems in the gas-phase, SOA from intermediate volatility compounds (IVOCs), and semi-volatile POA. Fire event $PM_{2.5}$ organic aerosol was estimated using both approaches.

Fires emit VOCs (toluene, xylenes, benzene, isoprene, and monoterpenes) that form SOA in both AE6 and VBS treatments. Semi-volatile SOA from all VOCs is aged in AE6 via an oligomerization pathway to nonvolatile form (Carlton et al., 2010). In the VBS, gas-phase semi-volatiles from anthropogenic VOCs (toluene, xylenes, benzene) are aged in the gas-phase to lower-volatility products (Koo et al., 2014; Robinson et al., 2007). The semi-volatile products from biogenic VOC (isoprene and monoterpenes) oxidation are not aged in the VBS treatment. Organic aerosol emitted from fires (typically referred to as POA) is treated as non-volatile but heterogeneously oxidized in AE6 (Simon and Bhave, 2012) and as semi-volatile organic compounds (SVOCs, $1 \leq C^* \leq 1000\ \mu g/m^3$) (May et al., 2013) with gas-phase oxidation in the VBS (Koo et al., 2014). In the CMAQ v5.0.2 VBS, primary SVOCs from biomass burning are largely distributed into the higher volatility bins (60%) with only 20% being allocated to the non-volatile bin (Woody et al., 2016). Some fraction of the primary SVOC oxidation products are moved to the secondary biogenic OA basis set (done to maintain accurate O:C ratios) where organic carbon continues to partition between the gas and aerosol phase but will no longer age. Additional intermediate volatility (IVOC) emissions thought to form SOA and to be missing from or mischaracterized in current emission inventories are included in the VBS treatment (but not AE6) based on scaling from the particulate biomass sector OA emissions (IVOC = 1.5 * biomass POA, where biomass POA = biomass primary SVOCs) (Robinson et al., 2007). Due to a lack of data for biomass burning, the assumed 1.5 scaling factor which is based on measurements from a diesel generator is a source of uncertainty. Other research indicates biomass burning may emit less IVOC per unit POA than diesel engines (Grieshop et al., 2009; Pye and Seinfeld, 2010).

CMAQ calculates photolysis rates by solving for the actinic flux from the two-stream approximation of the radiative transfer equation (Binkowski et al., 2007; Toon et al., 1989) for a waveband structure based on the FAST-J photolysis model (Wild et al., 2000). Light is attenuated based on simulated meteorological conditions and concentrations of gas and aerosol species such as O_3 and black carbon, respectively. Attenuation from aerosols uses a volume averaged mixing model to compute their optical properties. Each aerosol species is assigned a refractive index (Table S-1) such as black carbon, water, sulfate, organic and other insoluble species (Bond and Bergstrom, 2006; Chang and Charalampopoulos, 1990; Horvath, 1995). Assignments do not differentiate organic species between brown carbon and less absorbing organics because of uncertainties that include what organic species correspond to brown carbon, what refractive indices to use, and whether model physics accurately represent production and loss processes of brown carbon (Laskin et al., 2015). In CMAQ v5.0.2, all organic aerosol is therefore treated simply as dust (Table S-2).

Contribution from specific fire events were tracked using source sensitivity and source apportionment approaches. Daily emissions from the Wallow and Flint Hills fires tracked for contribution are shown in Table 2. The source sensitivity (brute force zero-out) approach involves comparing a baseline simulation with all emissions to a simulation with a fire removed from the emission input file (Cohan and Napelenok, 2011). The difference in model predicted air quality is considered the contribution from that fire. Source apportionment approaches track precursors and direct $PM_{2.5}$ emissions from specific fires (Wallow and Flint Hills) through the model chemical and physical processes to estimate their contribution to O_3 and $PM_{2.5}$. The Integrated Source Apportionment Method (ISAM) implemented in CMAQ for O_3 (Kwok et al., 2015)

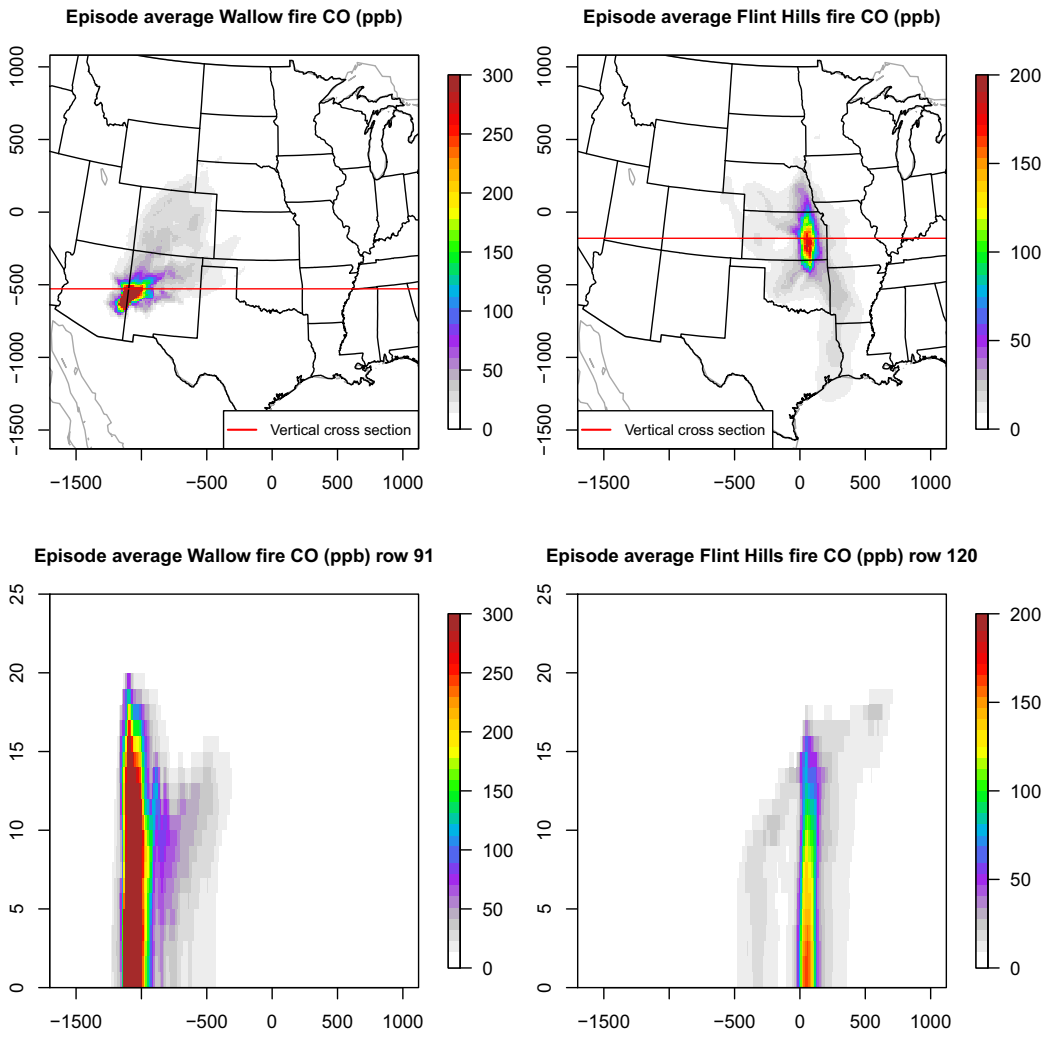

Fig. 1. Episode average surface layer CO impact from Wallow (left) and Flint Hills (right) fires. The solid line on the spatial plots indicate the row extracted for the vertical column shown in the bottom panels.

and $PM_{2.5}$ (Kwok et al., 2013) was used to track the contribution from each fire. Both source sensitivity and source apportionment approaches have been shown to capture impacts from specific sources (Baker and Kelly, 2014; Zhou et al., 2012) but source attribution using these two approaches can differ in cases where secondary pollutants are affected by highly non-linear chemical reactions (Kwok et al., 2013, 2015; Wang et al., 2009).

Actual fire impacts are qualitatively assessed using NOAA Hazard Mapping System (HMS) data (National Oceanic and Atmospheric Administration, 2016). HMS uses information from multiple satellites to provide an estimate of smoke density. The HMS product does not provide an estimate of surface layer O_3 or $PM_{2.5}$ impacts from all fires or specific fires but does provide a useful tool for assessing days where the Wallow or Flint Hills fires may have notable local to regional impacts. HMS plots used for this assessment are provided in the supporting information (Figures S3 and S4).

3. Results

Photochemical model predictions of domain-wide O_3 and largest components of $PM_{2.5}$ (sulfate ion, nitrate ion, organic carbon, and elemental carbon) compare well with surface level measurements made at rural locations during the periods modeled for the Wallow and Flint Hills fires. The domain-wide model performance is illustrated using multiple metrics including mean bias, mean error, median bias, and median error and shown for each pollutant in Table S-3. During the Wallow fire period the model slightly underestimates domain-wide O_3 and speciated $PM_{2.5}$. The Flint Hills period also has slightly underestimated O_3 and little bias related to speciated $PM_{2.5}$. These domain-wide metrics are generally consistent with other applications (Simon et al., 2012) and provides confidence that the modeling system is broadly providing a realistic chemical environment around the fires studied here. The model performs less well for specific monitors affected by the fire plumes and model results for these monitors are discussed in more detail below.

Two approaches were used for estimating the contribution from the Wallow and Flint Hills fires: 1) source sensitivity brute force zero-out of the fire emissions and 2) source attribution of the fire by difference between the baseline source apportionment simulation where all fires are tracked for contribution and subsequent source apportionment simulation where a specific (e.g., Wallow) fire event emissions are not included. Fire contribution using brute-force zero

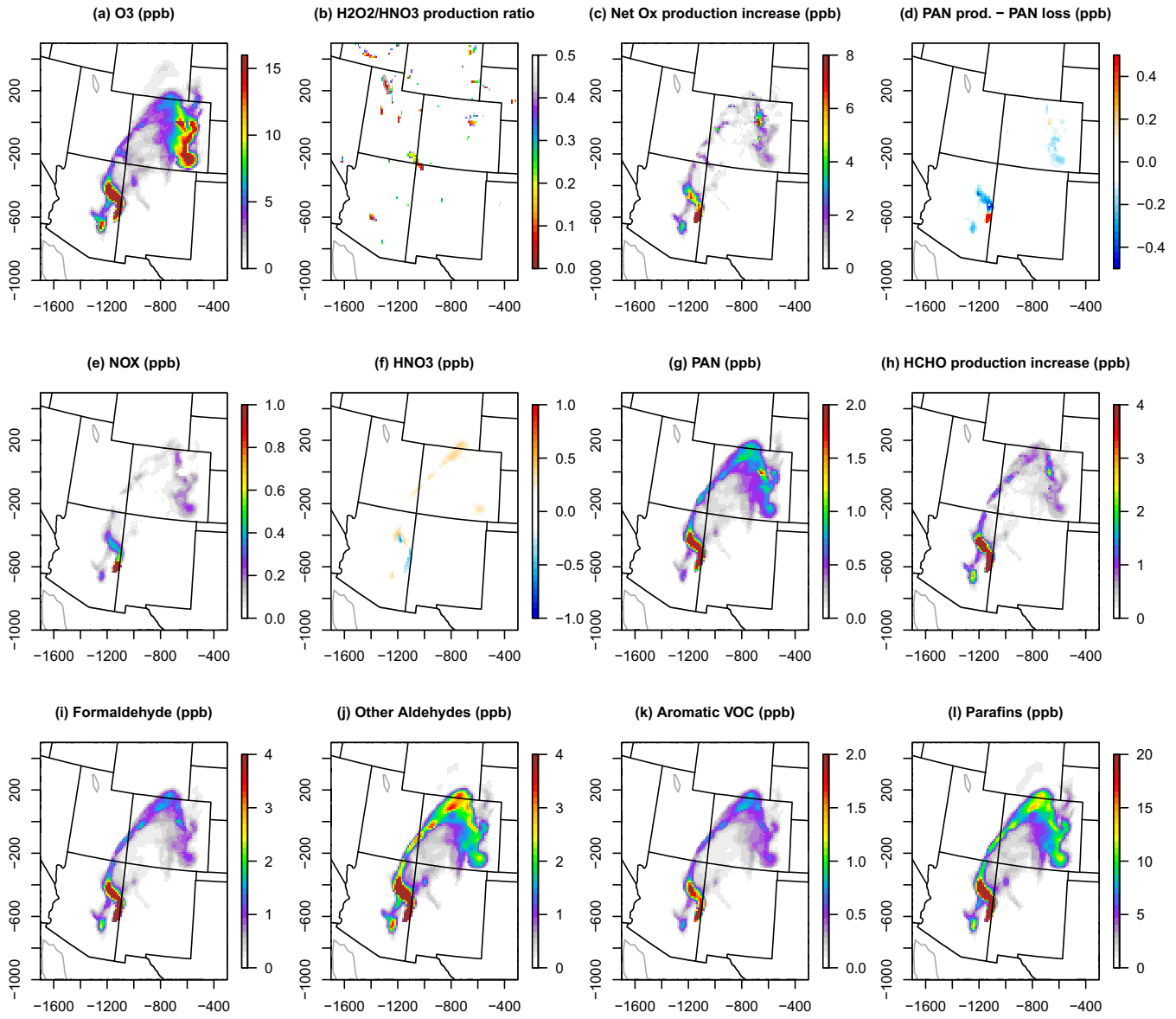

Fig. 2. Modeled Wallow fire contribution for June 5, 2011 at 19:00 UTC (2 p.m. local): O_3, bulk model H_2O_2/HNO_3 production ratio, O_x production, PAN production − PAN loss, NO_X, HNO_3, PAN, formaldehyde production, formaldehyde, other aldehydes, aromatic VOC, and parafins.

out and source apportionment were compared for episode peak primary and secondary pollutant impacts (Figures S-5 through S-8). The spatial pattern and magnitude of peak downwind contribution to primary pollutants such as CO and primary $PM_{2.5}$ species and secondary pollutants such as O_3 and $PM_{2.5}$ ammonium sulfate and nitrate are consistent between brute-force zero out and source apportionment approaches. Some differences do exist between these approaches which is expected, especially for secondarily formed pollutants since source apportionment is not intended to estimate changes in air quality due to sensitivities (e.g., O_3 titration due to NO_X emissions) (Kwok et al., 2015).

The period average modeled CO attributable to each fire is shown in Fig. 1. CO is highest near the fire and decreases as distance from the fire increases in the direction of prevailing winds during the time period modeled. Fig. 1 also shows a vertical cross-section of the period average CO attributed to each fire. Both fires have fairly uniform distributions of CO from the surface to the top of the surface mixing layer. The Wallow fire impacts extend from the surface to layers 18 and 19 which corresponds to approximately 3–4 km above ground level and the Flint Hills fire plume extends from the surface to layers 15 and 16 which are approximately 2–2.5 km above ground level. This fairly uniform fire impact through the surface mixing layer is likely a combination of the model typically well-mixing pollutants within the boundary layer and the distribution of fire emissions from the surface to plume top using the Briggs approach for plume rise estimation.

3.1. O_3 impacts

The contribution to modeled ambient pollutants from the Wallow fire are shown in Fig. 2 for June 5, 2011 at 19:00 UTC (2 p.m. local) to illustrate local to regional scale O_3 impacts. These plots show the change in mixing ratio of key species as the difference of the base case simulation with the Wallow fire emissions minus the

sensitivity simulation with the Wallow fire emissions removed. The Wallow fire modeled impacts on O_3 shown in Fig. 2a are elevated both near the fire and downwind along the Rocky Mountain front-range in eastern Colorado due to long range transport of O_3 and precursors from fire emissions on the previous day. A large increase in O_3 production near the fire is caused by increased availability of both NO_X and highly reactive VOC in the fire plume. Table 1 shows that 7.8% of the fire TOG emissions are estimated to be aldehydes (ALD2) and higher aldehydes (ALDX) and these species react rapidly to form peroxyacyl radicals which then react with NO_2 to form PAN and higher PAN analogues. Fig. 2g shows a large increase in the PAN mixing ratio near the fire and smaller PAN increases downwind of the fire in Colorado. Fig. 2f also shows reductions in nitric acid (HNO_3) near the fire compared to the simulation with no fire emissions, i.e., the increased VOC in the fire plume was sufficiently large to cause a shift in the conversion of NO_2 from relatively unreactive HNO_3 to PAN. Because PAN has an atmospheric lifetime of several hours to several days (Fischer et al., 2014) before decomposing to form peroxyacyl radicals and NO_2, PAN acts as a reservoir of reactive NO_2 that can be transported hundreds of km downwind of the fire (Baylon et al., 2015). Fig. 2d shows the net change in production of PAN with large increases in PAN production near the fire and increased PAN decomposition downwind of the fire and in eastern Colorado. Temperature enhancements from the fire itself occur in close proximity to the fire and typically reduce to levels of the surrounding ambient air within minutes, meaning it is unlikely that this would have a strong impact on PAN formation at the temporal and spatial resolution of this model application (Clements, 2010).

Fig. 2b shows the ratio of production of hydrogen peroxide (H_2O_2) to production of HNO_3 at 19:00 UTC. Previous work has described the importance of radical termination reactions that produce H_2O_2 and HNO_3 and evaluated their use as indicators of the sensitivity of O_3 to VOC and NO_X (Kleinman, 1991, 1994; Sillman et al., 1990). Sillman (1995) proposed that the ratio of H_2O_2/HNO_3 concentrations of about 0.3–0.5 demarks the transition of the daytime peak O_3 concentration from VOC sensitive to NO_X sensitive conditions. Tonnesen and Dennis (2000) used an analysis of radical propagation to show that the ratio of H_2O_2/HNO_3 production rates is a very robust indicator of the sensitivity of the production rates of odd oxygen (O_X) and O_3 to changes in VOC and NO_X, with ratios greater than 0.12 being strongly NO_X limited. Fig. 2b shows that the O_3 production in the fire plume and in most areas of the model domain are strongly NO_X limited for O_3 production at 19:00 UTC, with the exception of urban centers and areas such as the Four Corners region that have large industrial sources of NO_X emissions. The increased transport and subsequent decomposition of PAN, including eastern Colorado, results in increased NO_X availability and increased O_3 production in these NO_X limited areas.

Fig. 2i and j show large increases in formaldehyde (HCHO) and higher aldehydes (ALD2 and ALDX), respectively, with increases of 25 ppb in HCHO and 20 ppb in aldehydes near the fire, and increases greater than 2 ppb in northern and eastern Colorado. As noted above, aldehydes are a large component of the fire emissions and HCHO is 8.4% of fire TOG emissions. In addition to being emitted directly by the fire, aldehydes are also produced in the oxidation reactions of other VOC species including aromatics, olefins and parafins which are also enhanced in the fire plume as shown in Fig. 2k for aromatics and Fig. 2l for parafins. The CMAQ process analysis tool was used to calculate hourly average secondary production of HCHO in VOC oxidation reactions in both the base case and zero fire emissions simulation. Fig. 2h shows increases in secondary production of HCHO and production of O_X in the simulation with the fire emissions on July 5 at 19:00 GMT. Production rates of HCHO near the fire are greater than 20 ppb/hour, and HCHO production is enhanced by more than 1 ppb/hour in rural areas in northern and eastern Colorado and more than 2 ppb/hour in the Denver area. For comparison, model simulated HCHO production rates in the southwestern U.S. are typically less than 2 ppb/hour in rural areas and in the range of 2–6 ppb/hour in urban areas (Figure S-9). Fig. 2c shows that the O_X production rate increased by more than 10 ppb/hour in the Denver area at 19:00 GMT. The production of O_X is calculated as the net production during a modeled one hour time step and thus reflects the combined production of O_3 and net oxidation of NO to NO_2. The area of greatest increase in production of HCHO and O_X in the Denver urban core area coincides with the area that the H_2O_2/HNO_3 production ratio indicates is highly radical limited and VOC sensitive. Thus, the increased O_X production and fire attributable O_3 mixing ratio in the Denver area is primarily a result of transport of VOC in the fire plume, while the increase in O_3 mixing ratios in NO_X limited areas is primarily a result of transport of PAN and its subsequent decomposition to release NO_X.

Using a photochemical transport model to isolate the impacts of fire plumes provides an opportunity to directly quantify the modeled O_3 production relative to CO from a fire. Carbon monoxide is considered a generally conserved tracer from emissions sources such as fires and observations of the excess ratio ($\Delta O3/\Delta CO$) in fire plumes have been used to characterize chemical production of O_3 in the plume (Jaffe and Wigder, 2012; Vakkari et al., 2014). The excess ratio in the Wallow and Flint Hills fire plumes was estimated

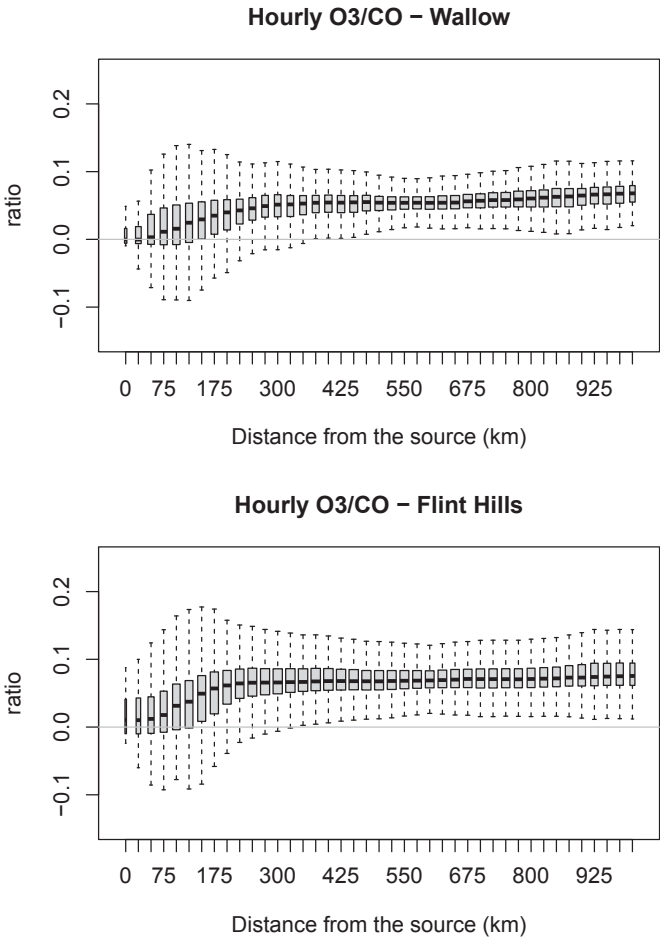

Fig. 3. Hourly modeled O_3:CO enhancement ratios are shown as a function of distance from the Wallow and Flint Hills fires. Centerline shows the median values, boxes show the 25th and 75th percentiles and whiskers extend to 1.5 times the interquartile range.

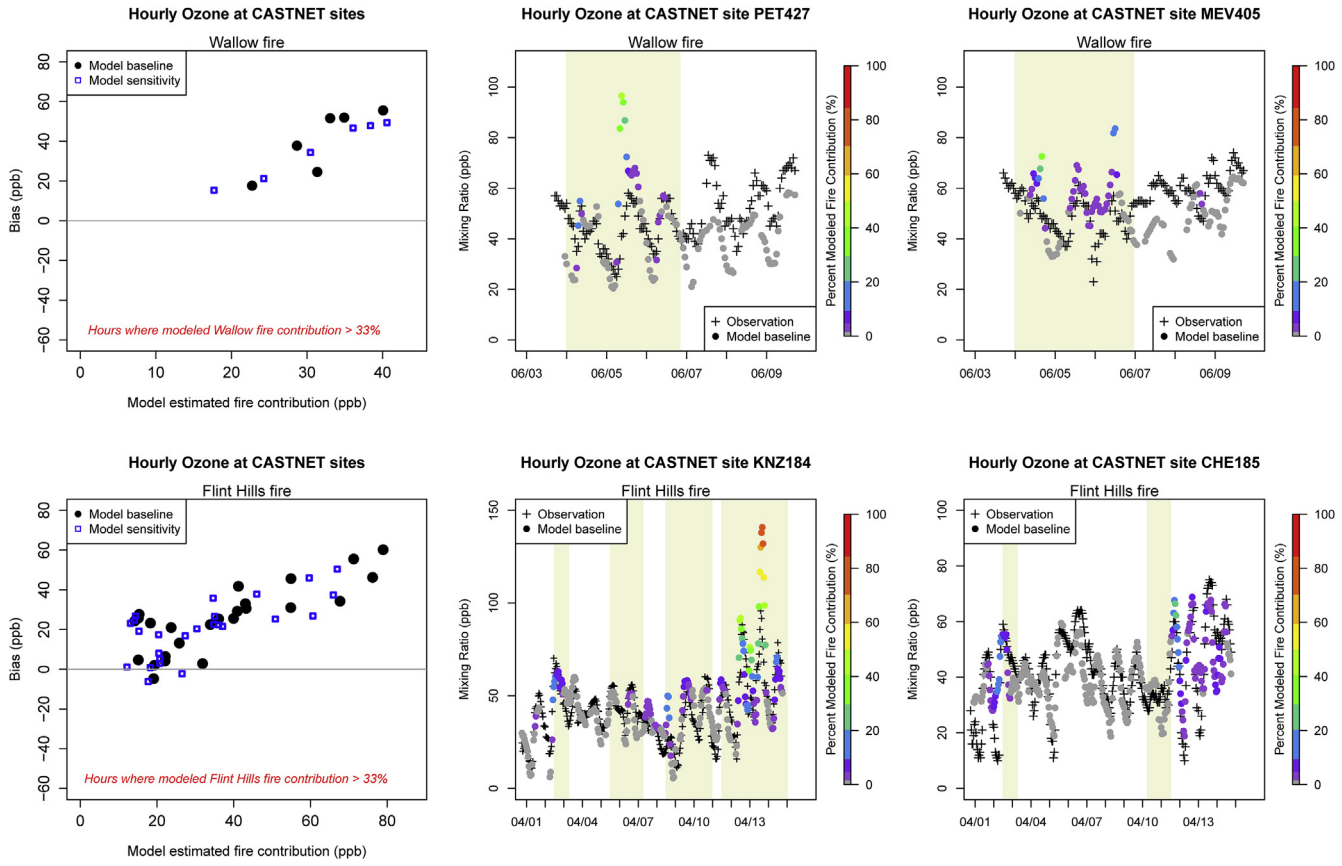

Fig. 4. Hourly modeled fire contribution paired with bulk model O_3 bias at rural CASTNET monitors. The shaded areas of the time series plots indicate days with possible Wallow or Flint Hills fire impacts based on HMS data. The HMS data does not provide ground-level O_3 mixing ratios and only provides an indication of possible fire impact. The model sensitivity is the simulation where solar radiation and photolysis rates are more aggressively attenuated by modeled organic aerosol.

using the source sensitivity (brute-force zero-out of fire emissions) approach. Fig. 3 shows ΔO3/ΔCO as a function of distance from the fire. The enhancement ratios are smallest near fires where emissions are freshest. The median ratio gradually increases out to 150 km from the fire and levels off as distance from the fire and plume age increases. The range of ΔO3/ΔCO modeled for these fires (−0.054 to 0.184) is generally consistent with those made in observation based assessments reported for fire impacts with plume ages up to 5 days (Jaffe and Wigder, 2012). It is important when interpreting this comparison to note these observations represent a very small subset of fire impacts in the atmosphere and observed plume age is often difficult to constrain which makes direct comparison with these model estimates problematic. It is likely that the enhancement ratios presented in literature represent a small subset of all fires and even a subset of the fires samples in the reported studies and many observed O_3 enhancement ratios could be outside these reported values. Observation based ratios represent a change in O_3 divided by the change in CO in order to differentiate fire related enhancements from other sources. The model applications use source attribution to differentiate fire impacts from other sources so a difference between current and subsequent (sequentially successive) values is not needed. Negative ratios represent times where O_3 production was inhibited (e.g., smoke reduced photolysis or nighttime conditions) or where O_3 was removed (e.g. destroyed chemically or deposited to the surface) faster than CO. Modeled source sensitivity rather than source apportionment results are compared with ambient enhancement ratios to capture the negative ratios where O_3 is removed more quickly than CO. Source apportionment is not designed to capture negative O_3 production thus only directly applicable where O_3 production outpaces removal processes.

This enhancement ratio comparison provides some indication that the photochemical model captures the range of observed O_3 production and removal compared to a conserved tracer but does not show whether the model is over or under-estimating O_3 impacts from these fires. Model performance of hourly O_3 at rural Clean Air Status and Trends Network (CASTNET) monitors is examined where the model predicts a fire impact greater than a threshold (33% fire contribution) to emphasize modeled fire impacts in the model performance evaluation at locations (largely rural) that would have less influence from other sources. A contribution threshold is used to subset hours and locations where the fire would most impact model performance. Fig. 4 shows model (bulk: total O_3 from all sources not just fires) bias compared to model estimated fire contribution. A time series showing O_3 observations and model predicted O_3 shaded by percent contribution from the Wallow or Flint Hills fire is also shown for 2 sites in proximity to these fires. The time series plots are shaded for days that may be influenced by these fires based on a visual examination of HMS data (Figures S-3 and S-4). The HMS data shows an approximate smoke plume location as a qualitative indicator of fire impact but does not provide information about surface level O_3 impacts. For both Wallow and Flint Hills fires, the model tends to overestimate O_3 nearest the fire. This comparison has the most meaning at monitors close to the fire because monitors further downwind experience greater influence from other sources that affect model performance. Some of this over-prediction tendency may be related to the modeling system misplacing the smoke

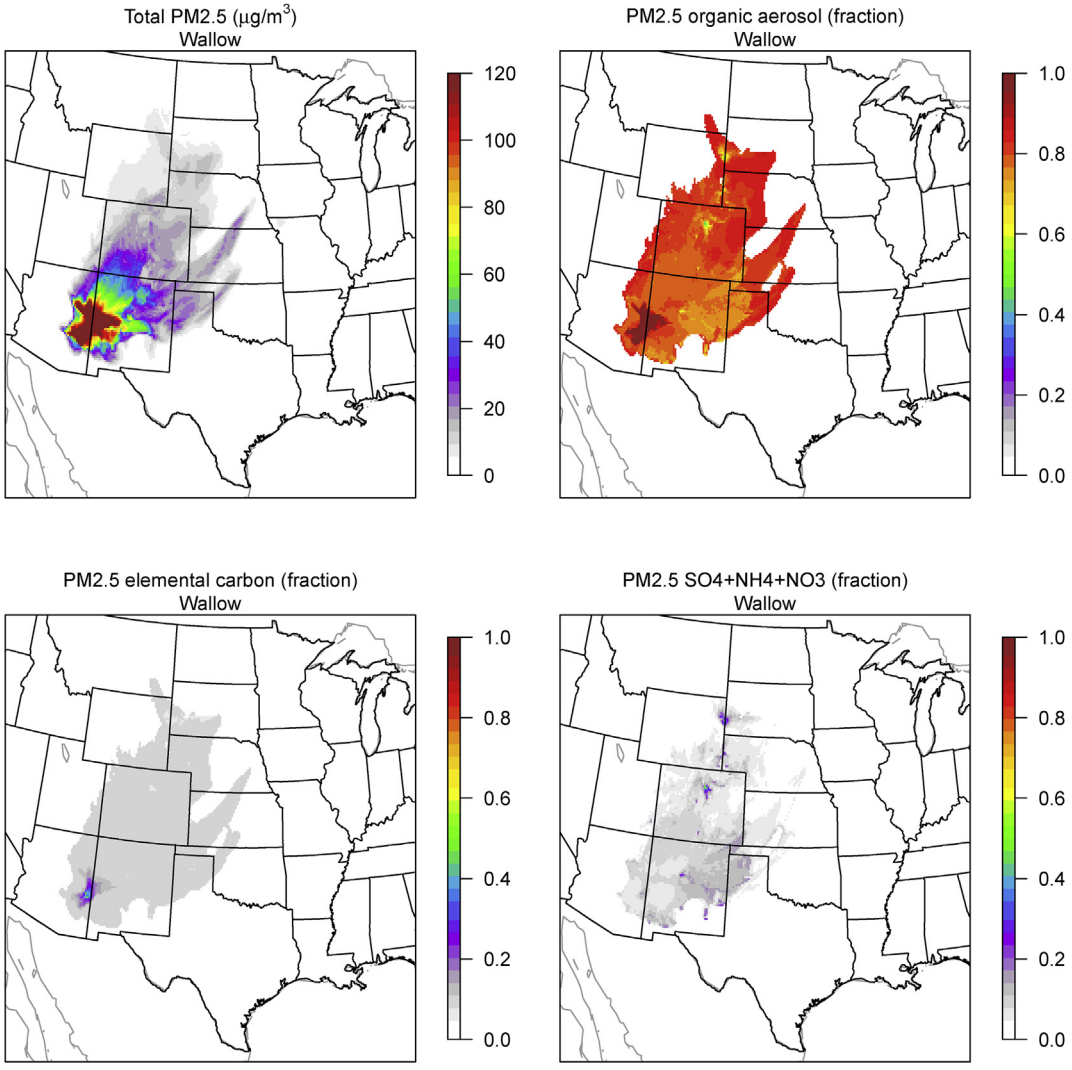

Fig. 5. Episode maximum hourly impacts from the Wallow fire to modeled $PM_{2.5}$. The percent composition of organic aerosol, elemental carbon, and the sum of ammonium, sulfate, and nitrate ions are also shown.

plume at surface monitors that did not actually get impacts by these fires, especially for the Wallow fire where the 12 km sized grid cells are likely not capturing some of the complex terrain effects on plume transport and dispersion in that area. Further, surface overestimates may also be related to possible over-dilution of lofted fire plumes though the boundary layer as Fig. 1 shows persistent well-mixed fire impacts throughout the surface mixing layer. Without coincident surface and upper air measurements the vertical extent of the plume is difficult to constrain.

The modeled O_3 contributions may be over-predicted because radiative feedbacks (where smoke reduces photolysis rates) in CMAQ v5.0.2 are largely driven by black carbon with less impact from organic carbon species, which dominate modeled fire PM composition. Jiang et al. (2012) have shown that a regional scale photochemical grid model with coupled meteorological and aerosol feedbacks reduced O_3 production in the fire plume due to reduced photolysis from smoke. Organic aerosol attenuates photolysis rates in CMAQ v5.0.2 as if it were dust and relatively non-absorbing, thus potentially overestimating photolysis rates (Table S-2). We performed a sensitivity simulation in which organic aerosol species were given refractive indices consistent with black carbon to more aggressively attenuate photolysis (Bond and Bergstrom, 2006; Chang and Charalampopoulos, 1990). Maximum hourly predicted O_3 decreases near the fire events and regionally as a result of this sensitivity simulation (see Figure S-10), typically less than 10% regionally. The sensitivity simulation showed improvements in model performance but did not remove the over-prediction and suggests other aspects of the modeling system also contribute to over-predictions (see Fig. 4). Model performance could be related to numerous aspects of the modeling system: emissions estimates, NO_Y and VOC speciation of emissions, temporal profiles, photolysis characterization, plume rise, and grid resolution. The reactivity of the VOC mixture in the fire emissions should also be further evaluated. Our results above and in Fig. 2h showed large secondary production of HCHO in the fire plume, and if observations of HCHO and higher aldehydes in fire plumes are assumed to be caused only by emissions, the fire emissions could be substantially overestimated for these highly reactive VOC species.

3.2. Particulate matter impacts

Figs. 5 and 6 show the modeled maximum hourly $PM_{2.5}$ impacts from these fire events along with fractional contribution of primary organic carbon, elemental carbon, and the sum of ammonium,

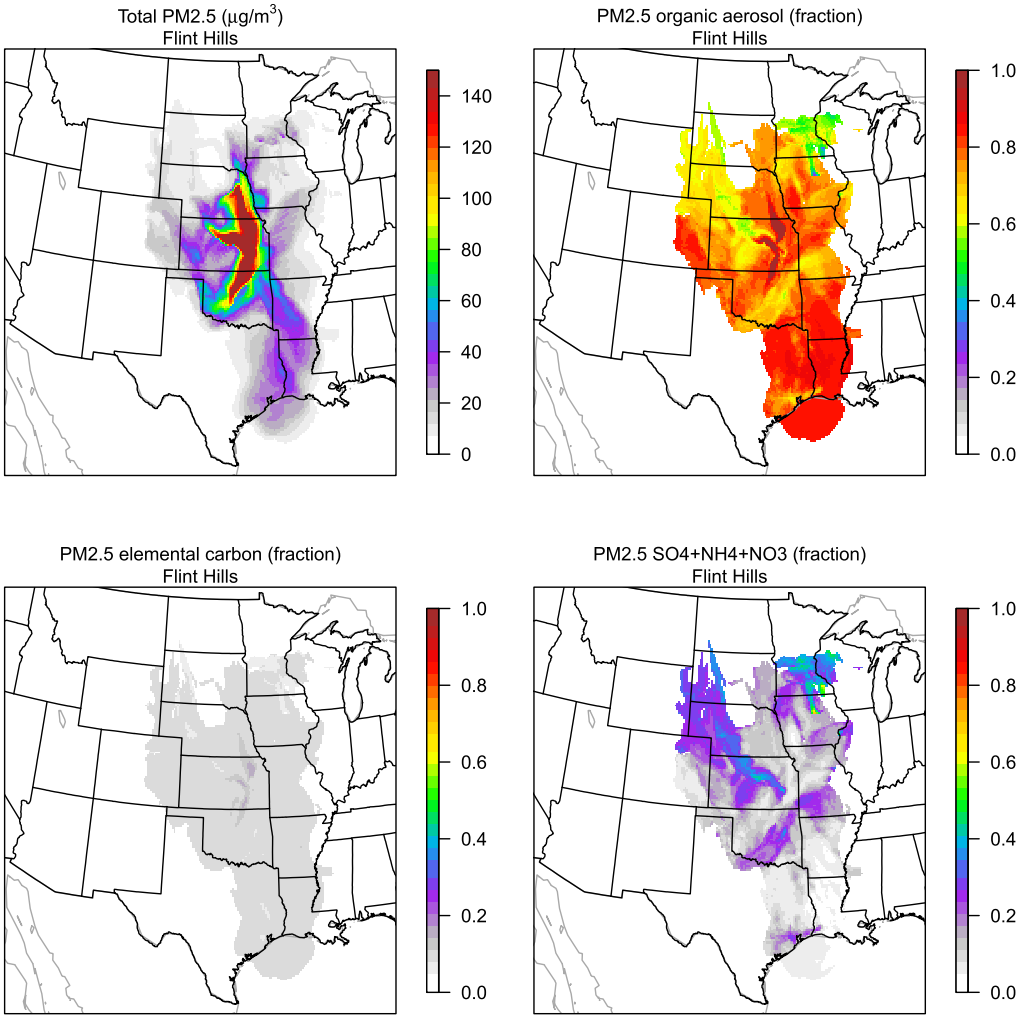

Fig. 6. Episode maximum hourly impacts from the Flint Hills fire to $PM_{2.5}$. The percent composition of organic aerosol, elemental carbon, and the sum of ammonium, sulfate, and nitrate ions are also shown.

sulfate, and nitrate ions using the baseline AE6 aerosol approach. The largest downwind component of fire $PM_{2.5}$ is organic aerosolmass, which is the largest component of the primary $PM_{2.5}$ emissions based on the source profile used here (Table 1). The differences between these fires in percent chemical contribution of ammonium, sulfate, and nitrate ions is likely due to the Flint Hills fire being in closer proximity to large ammonia emissions sources as compared with the Wallow fire. The total organic aerosol amount and relative contribution from different forms of $PM_{2.5}$ changes when $PM_{2.5}$ organic aerosol emissions get treated as semi-volatile (Konovalov et al., 2015). CMAQ was applied using the standard option (AE6) of estimating SOA with traditional biogenic and aromatic precursors and treating POA as non-volatile and also using the standard VBS approach that includes traditional SOA formation but treats POA as volatile, ages some of the SOA species, and includes SOA from IVOC emissions.

Hourly maximum $PM_{2.5}$ organic aerosol contribution is shown for each fire event in Fig. 7 using the standard AE6 aerosol treatment in CMAQ. The difference in maximum hourly $PM_{2.5}$ organic aerosol contribution is shown between the standard AE6 simulation, CMAQ volatility basis set approach and the VBS sensitivity where biogenic SOA is aged. The CMAQ-VBS approach results in lower OA near these fires and regionally downwind since a portion of the semi-volatile POA in the VBS treatment is present in the gas phase. However, the VBS sometimes estimates higher OA than AE6 in close proximity to the Flint Hills fire event. The higher OA estimates using the VBS approach are sporadic and tend to be in close proximity to fresh emissions where OA concentrations are high, conditions which favor semi-volatile partitioning to the particle phase. As the plume is transported downwind the VBS often shows lower impacts for the Flint Hills fire as OA concentrations diminish and particle phase semi-volatile POA partitions to the gas phase. Since both approaches estimate secondary organic aerosol from traditional aromatic and biogenic VOC, the higher OA estimated near the Flint Hills fire is likely due to additional emissions introduced into the model in the form of IVOCs, which in CMAQ-VBS produce biogenic SOA when oxidized and this effect is amplified when biogenic SOA is aged (Fig. 7). There also appears to be an influence of ambient temperatures on partitioning of semi-volatile POA, as cooler ambient temperatures during the Flint Hills fire allowed for more semi-volatile POA to remain in the particle phase whereas the warmer ambient temperatures during the Wallow fire

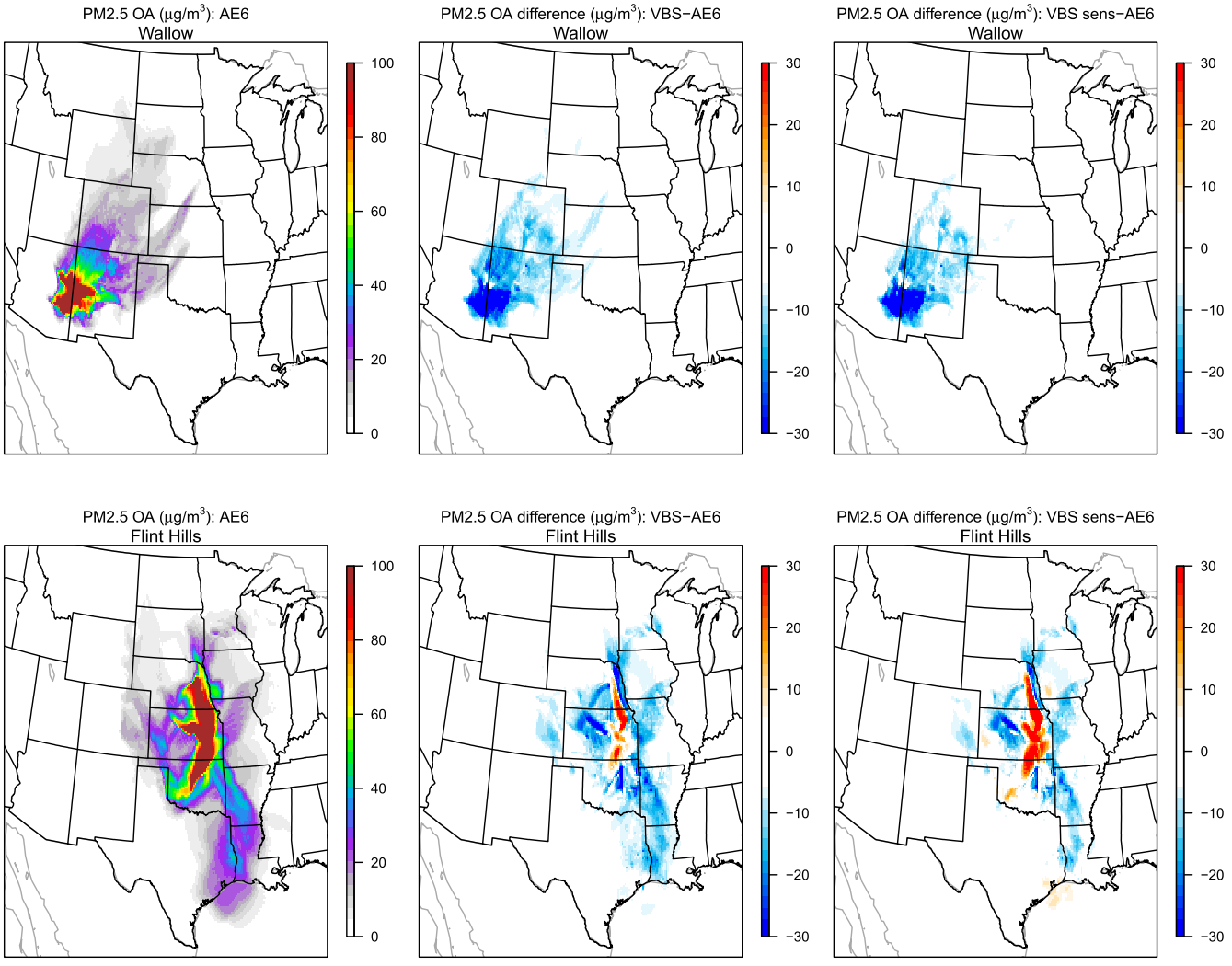

Fig. 7. Maximum hourly impacts from Wallow (top row) and Flint Hills (bottom row) fires to modeled $PM_{2.5}$ organic aerosol. The difference between the AE6, standard VBS, and VBS with secondary biogenic SVOC aging simulations are also shown. Cool colors indicate less $PM_{2.5}$ organic aerosol contribution with the sensitivity simulation.

evaporated a higher proportion of POA to the gas phase.

Fig. 8 shows hourly maximum primary OA estimated by the AE6 and VBS approaches for both fires, the maximum hourly SOA from aromatic VOC, and maximum hourly SOA from biogenic VOC. The VBS estimate of biogenic SOA also includes additional SOA from IVOC emissions and aged POA. The VBS approach results in a larger percentage of OA as SOA compared to AE6 but generally results in much lower OA regionally due to the semi-volatile POA. The increased fraction of secondary OA to total OA is consistent with other studies treating primarily emitted OA from fires as semi-volatile (Konovalov et al., 2015). Many implementations of the VBS including the approach used here do not include aging of biogenic SVOCs because this led to model overestimates of OA in rural areas or was considered too unconstrained (Pye and Seinfeld, 2010). Whether this type of treatment is appropriate for fires should be the focus of future research. A sensitivity simulation was applied for each fire event where the CMAQ VBS was modified to age secondary biogenic SVOCs similarly to secondary anthropogenic SVOCs (Ahmadov et al., 2012). This biogenic aging sensitivity resulted in higher estimates of OA from the Wallow fire event although regional OA totals are still lower for this fire than those with the AE6 approach where OA is largely primary and non-volatile (Fig. 7). The VBS sensitivity where the secondary biogenic basis set is aged due to OH reaction results in total OA estimates notably larger than that estimated by AE6 nearest the Flint Hills fire but often lower further downwind due to reasons described earlier.

Published enhancement ratios of organic aerosol to CO provide little insight as some studies show $PM_{2.5}$ enhancement ratios increasing with plume age (Ortega et al., 2013; Vakkari et al., 2014) while another shows both decreasing and no change with plume age (Forrister et al., 2015; May et al., 2015; Ortega et al., 2013). Modeled hourly $PM_{2.5}$ organic aerosol to CO ratios (Figure S-11) differ from published values in that often removal processes outpace production resulting in negative values. Positive modeled enhancement ratios are typically below 0.5 g/g but range up to ~1 g/g which is larger than reported values (between 0 and ~0.3 g/g) but reported values are not robust and likely do not capture the range of ambient OA production with respect to CO (Forrister et al., 2015; May et al., 2015; Vakkari et al., 2014). Model performance for bulk estimates of chemically speciated $PM_{2.5}$ at rural monitors part of the Interagency Monitoring of Protected Visual Environments (IMPROVE) network is examined where the model predicts an

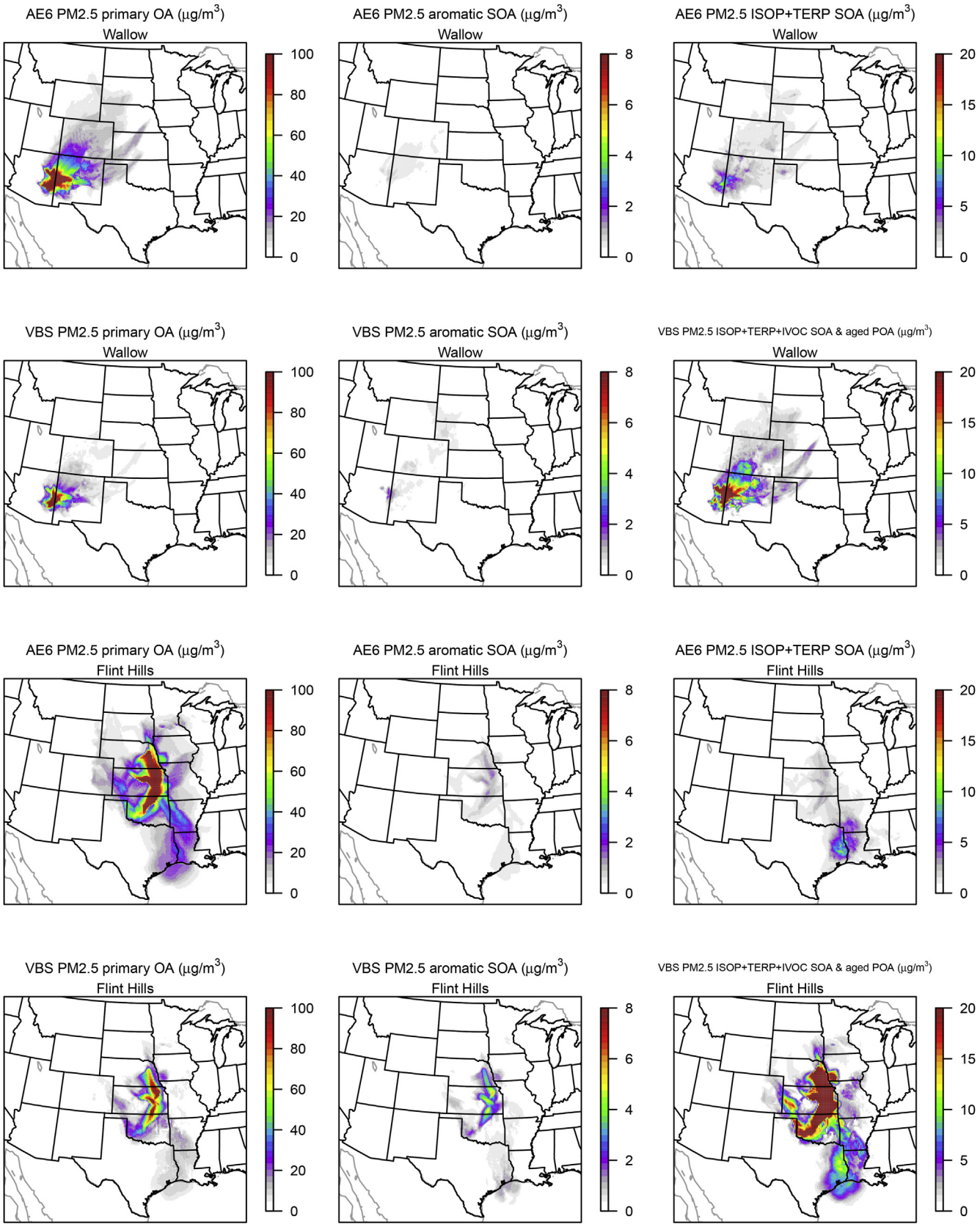

Fig. 8. Episode maximum hourly modeled $PM_{2.5}$ primary (left column) and secondary organic aerosol from each fire using AE6 and standard VBS methods. Aromatic SOA is shown in the middle column and biogenic SOA in the right column.

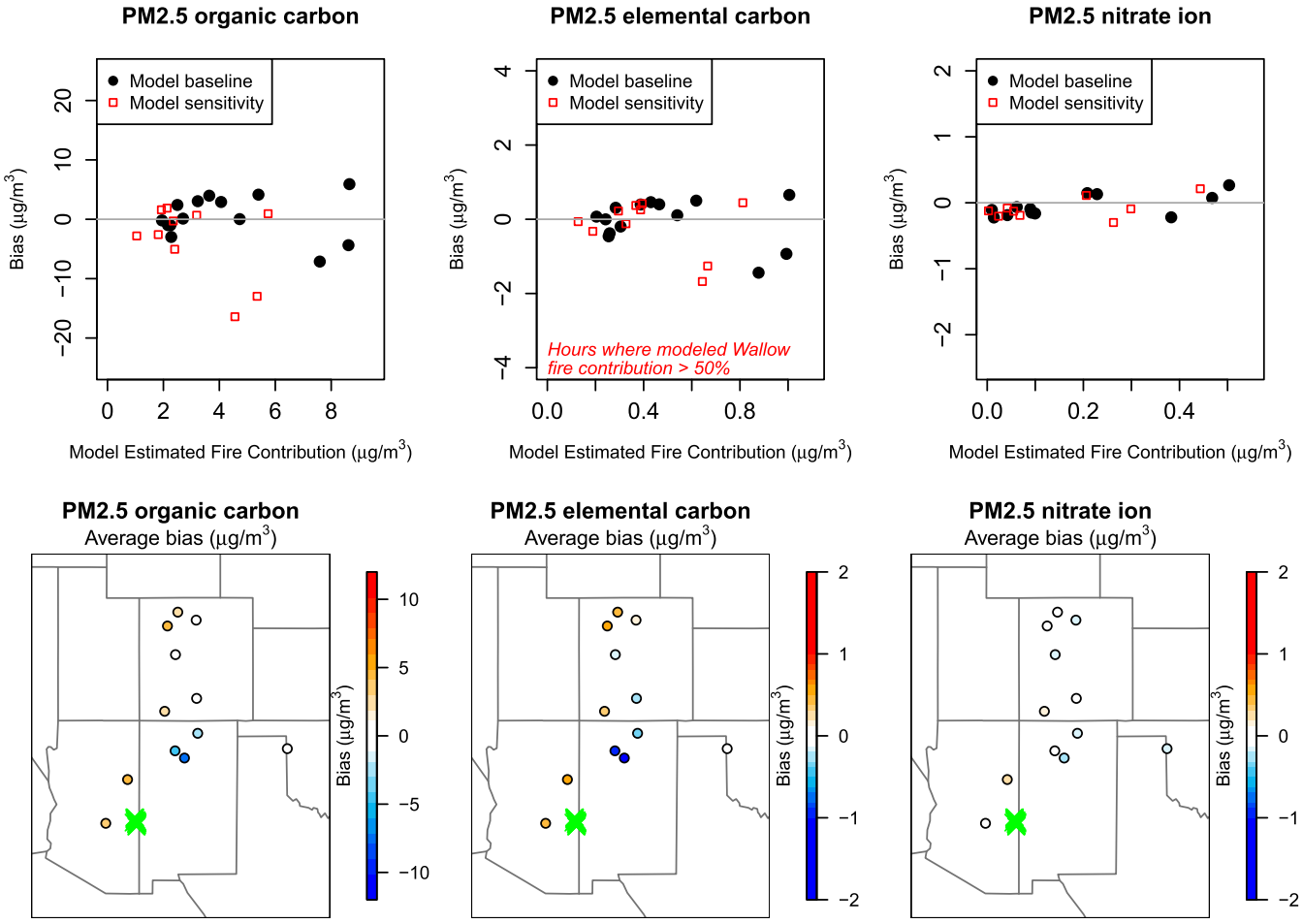

Fig. 9. Daily averaged modeled Wallow fire contribution paired with bulk model speciated $PM_{2.5}$ bias at rural IMPROVE monitors (top row). The average model bias is shown by monitor (bottom row). Warm colors indicate a model tendency toward over-prediction and cool colors indicate under-prediction. The "X" symbols show modeled fire centroid location. The model sensitivity represents the standard VBS simulation.

impact (30% Flint Hills fire or 50% Wallow fire contribution to OC) from one of the fire events tracked for contribution (Figs. 9 and 10). Bulk model performance is only partially a function of these fire events since other sources contribute to some degree to the model estimates, especially as distance from the fire increases. However, this comparison can provide some indication about whether the model tends to over or under-estimate on days where the model predicts a large fire contribution to a monitor. Both fires show over-estimates of organic and elemental carbon at sites in close proximity to the fires (Figs. 9 and 10). However, the closest IMPROVE site (TALL1) to the Flint Hills fires on the days with highest HMS smoke plume density in eastern Kansas did not report $PM_{2.5}$ elemental or organic carbon which further complicates this comparison. It is possible the surface measurement stations missed the highest impacts from these fires.

Ammonium sulfate (not shown) and ammonium nitrate are better predicted although small ammonium nitrate under-predictions occur for the Flint Hills fire. Model performance for speciated $PM_{2.5}$ is generally similar when using the CMAQ VBS approach although organic carbon tends to be underestimated where strongly influenced by the Wallow fire and still over-estimated where influenced by the Flint Hills fire (Fig. 8). The VBS method in CMAQ tends to result in slightly lower estimates of non-organic aerosol species which is the result of POA evaporation in the VBS changing the bulk PM size distribution which increases dry deposition velocities for all $PM_{2.5}$ species (Koo et al., 2014). The overestimation of organic aerosol at sites downwind in proximity to the Flint Hills fire suggests the $PM_{2.5}$ emission factor used here for grasses may be too high. Similar to O_3, in addition to errors related to fire emissions and chemistry treatment, over-predictions may come from errors in plume rise, plume transport, simulated meteorological conditions, or some combination of these issues.

4. Conclusions & future direction

Hourly O_3 and daily average $PM_{2.5}$ organic carbon at rural monitors with high modeled impacts from these fires suggest model overprediction. A sensitivity analysis where photolysis rates are more aggressively attenuated by particulate carbon species reduces downwind surface level hourly O_3 and improves model performance at rural monitors compared to the baseline simulation. This shows the importance of light attenuation on O_3 production in fire plumes and highlights the need for more specific information about the optical properties of brown carbon since that is a large component of modeled aerosol from these fires. An alternative simulation where organic aerosol is treated as semi-

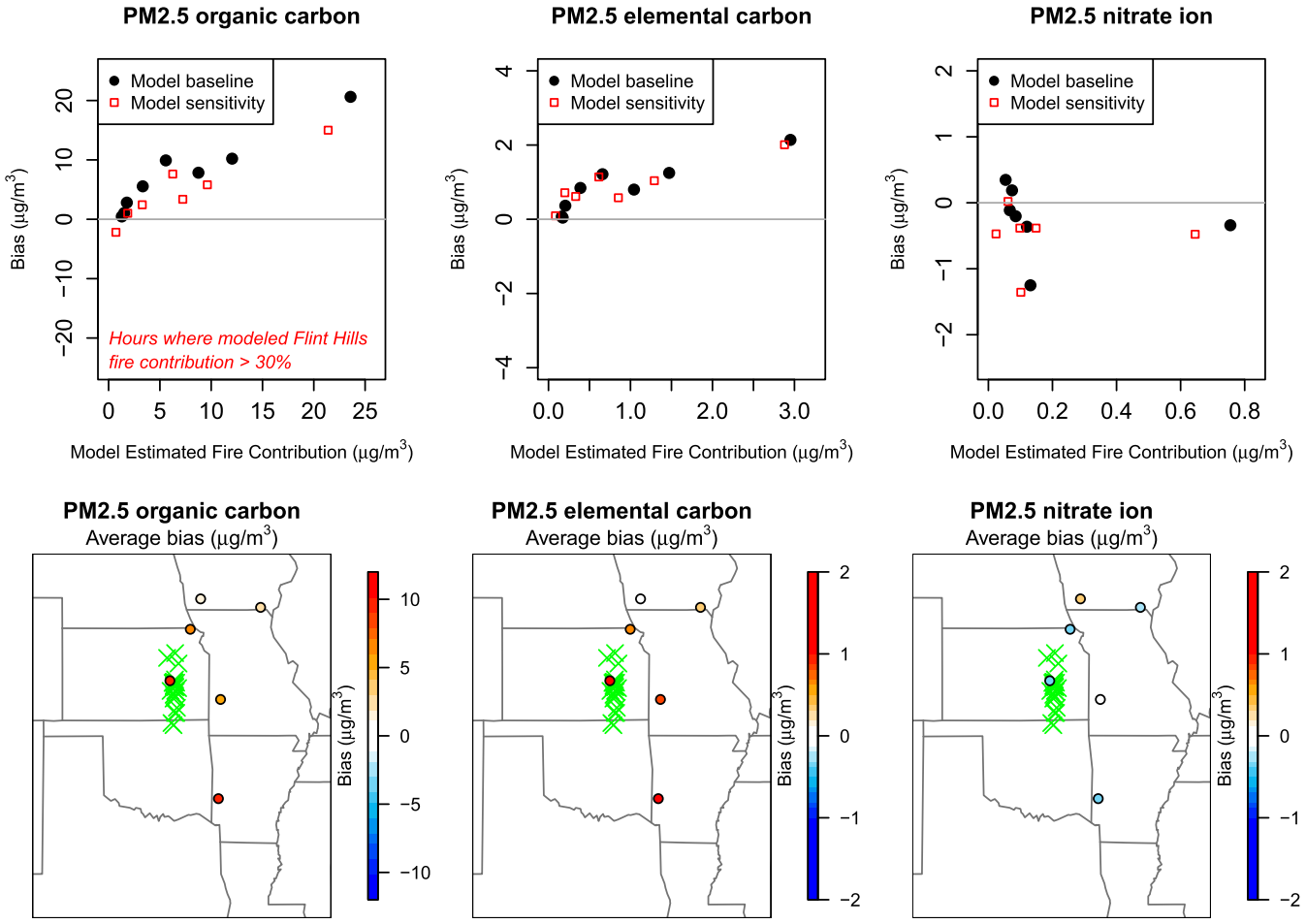

Fig. 10. Daily averaged modeled Flint Hills fire contribution paired with bulk model speciated $PM_{2.5}$ bias at rural IMPROVE monitors (top row). The average model bias is shown by monitor (bottom row). Warm colors indicate a model tendency toward over-prediction and cool colors indicate under-prediction. The "X" symbols show modeled fire centroid location. The model sensitivity represents the standard VBS simulation.

volatile with the volatility basis set results in much lower organic aerosol contributions from these fires although some increases are seen relative to the baseline which may be related to aging or IVOC emissions assumptions. Further research is needed to better understand the application of the volatility basis set for biomass burning with respect to 1) the degree of POA volatility, 2) IVOC estimates, and 3) aging SVOCs. The optical properties of smoke and subsequent attenuation effects on chemistry and treatment of organic aerosol as semi-volatile highlight a few of many aspects of fire emissions and modeling that need better understanding and improvement so that models better capture primary and secondary pollutant impacts from fires.

More work needs to be done to better constrain model predictions of wildland fires to improve confidence in those predictions. Measurement studies are needed to ascertain the relative importance of direct fire emissions of HCHO and aldehydes compared to their secondary production from VOC oxidation in the fire plume. The source apportionment and sensitivity techniques used here to isolate fire impacts on downwind primary and secondary pollutants should be used to match modeled fire impacts with field study data. Measurements in well characterized fire plumes are currently fairly sparse, however additional critical data may be available from planned future local to regional scale wildfire plume measurement field studies including the Fire Influence on Regional and Global Environments Experiment (FIREX) and Fire and Smoke Model Evaluation Experiment (FASMEE) field campaigns. These field experiments along with other ongoing and coordinated efforts provide a unique opportunity to obtain surface and upper air measurements of specific fires to better constrain fire emissions and the physical and chemical evolution of smoke plumes.

Disclaimer

Although this work was reviewed by EPA before publication, it may not necessarily reflect official Agency policy.

Acknowledgements

The authors would like to recognize the contributions of Venkatesh Rao, James Beidler, Ana Rappold, Melanie Wilson, Pat Dolwick, Norm Possiel, Rich Scheffe, Brian Gullett, Matt Landis, Luxi Zhou, Allan Beidler, Chris Allen, and Lara Reynolds.

Appendix A. Supplementary data

Supplementary data related to this article can be found at http://dx.doi.org/10.1016/j.atmosenv.2016.06.032

References

Ahmadov, R., McKeen, S., Robinson, A., Bahreini, R., Middlebrook, A., Gouw, J.D., Meagher, J., Hsie, E.Y., Edgerton, E., Shaw, S., 2012. A volatility basis set model for summertime secondary organic aerosols over the eastern United States in 2006. J. Geophys. Res. Atmos. 117, 1984–2012.

Akagi, S., Craven, J., Taylor, J., McMeeking, G., Yokelson, R., Burling, I., Urbanski, S., Wold, C., Seinfeld, J., Coe, H., 2012. Evolution of trace gases and particles emitted by a chaparral fire in California. Atmos. Chem. Phys. 12, 1397–1421.

Baker, K.R., Kelly, J.T., 2014. Single source impacts estimated with photochemical model source sensitivity and apportionment approaches. Atmos. Environ. 96, 266–274.

Bash, J., Baker, K.R., Beaver, M., 2016. Evaluation of improved land use and canopy representation in BEIS v3. 61 with biogenic VOC measurements in California. Geosci. Model Dev. 9, 2191–2207.

Baylon, P., Jaffe, D., Wigder, N., Gao, H., Hee, J., 2015. Ozone enhancement in western US wildfire plumes at the Mt. Bachelor Observatory: the role of NO x. Atmos. Environ. 109, 297–304.

Binkowski, F.S., Arunachalam, S., Adelman, Z., Pinto, J.P., 2007. Examining photolysis rates with a prototype online photolysis module in CMAQ. J. Appl. Meteorol. Climatol. 46, 1252–1256.

Bond, T.C., Bergstrom, R.W., 2006. Light absorption by carbonaceous particles: an investigative review. Aerosol Sci. Technol. 40, 27–67.

Bytnerowicz, A., Burley, J.D., Cisneros, R., Preisler, H.K., Schilling, S., Schweizer, D., Ray, J., Dulen, D., Beck, C., Auble, B., 2013. Surface ozone at the Devils Postpile National Monument receptor site during low and high wildland fire years. Atmos. Environ. 65, 129–141.

Cai, C., Kulkarni, S., Zhao, Z., Kaduwela, A.P., Avise, J.C., DaMassa, J.A., Singh, H.B., Weinheimer, A.J., Cohen, R.C., Diskin, G.S., 2016. Simulating reactive nitrogen, carbon monoxide, and ozone in California during ARCTAS-CARB 2008 with high wildfire activity. Atmos. Environ. 128, 28–44.

Carlton, A.G., Baker, K.R., 2011. Photochemical modeling of the ozark isoprene Volcano: MEGAN, BEIS, and their impacts on air quality predictions. Environ. Sci. Technol. 45, 4438–4445.

Carlton, A.G., Bhave, P.V., Napelenok, S.L., Edney, E.O., Sarwar, G., Pinder, R.W., Pouliot, G.A., Houyoux, M., 2010. Treatment of secondary organic aerosol in CMAQv4.7. Environ. Sci. Technol. 44, 8553–8560.

Chang, H., Charalampopoulos, T., 1990. Determination of the wavelength dependence of refractive indices of flame soot. In: Proceedings of the Royal Society of London A: Mathematical, Physical and Engineering Sciences. The Royal Society, pp. 577–591.

Clements, C.B., 2010. Thermodynamic structure of a grass fire plume. Int. J. wildland fire 19, 895–902.

Cohan, D.S., Napelenok, S.L., 2011. Air quality response modeling for decision support. Atmosphere 2, 407–425.

Diaz, J.M., 2015. Health Effects of Wildland Fire Smoke: Insight from Public Health Science Studies.

Fann, N., Fulcher, C.M., Baker, K., 2013. The recent and future health ьurden of air pollution apportioned across US sectors. Environ. Sci. Technol. 47, 3580–3589.

Fischer, E., Jacob, D.J., Yantosca, R.M., Sulprizio, M.P., Millet, D., Mao, J., Paulot, F., Singh, H., Roiger, A., Ries, L., 2014. Atmospheric peroxyacetyl nitrate (PAN): a global budget and source attribution. Atmos. Chem. Phys. 14, 2679–2698.

Forrister, H., Liu, J., Scheuer, E., Dibb, J., Ziemba, L., Thornhill, K.L., Anderson, B., Diskin, G., Perring, A.E., Schwarz, J.P., 2015. Evolution of brown carbon in wildfire plumes. Geophys. Res. Lett. 42 (11), 4623–4640.

Fountoukis, C., Nenes, A., 2007. ISORROPIA II: a computationally efficient thermodynamic equilibrium model for K+–Ca2+–Mg2+–Nh(4)(+)–Na+–SO42–NO3–Cl–H2O aerosols. Atmos. Chem. Phys. 7, 4639–4659.

Garcia-Menendez, F., Hu, Y., Odman, M.T., 2014. Simulating smoke transport from wildland fires with a regional-scale air quality model: sensitivity to spatio-temporal allocation of fire emissions. Sci. Total Environ. 493, 544–553.

Garcia-Menendez, F., Hu, Y., Odman, M.T., 2013. Simulating smoke transport from wildland fires with a regional-scale air quality model: sensitivity to uncertain wind fields. J. Geophys. Res. Atmos. 118, 6493–6504.

Grieshop, A., Logue, J., Donahue, N., Robinson, A., 2009. Laboratory investigation of photochemical oxidation of organic aerosol from wood fires 1: measurement and simulation of organic aerosol evolution. Atmos. Chem. Phys. 9, 1263–1277.

Henderson, B., Akhtar, F., Pye, H., Napelenok, S., Hutzell, W., 2014. A database and tool for boundary conditions for regional air quality modeling: description and evaluation. Geosci. Model Dev. 7, 339–360.

Horvath, H., 1995. Size segregated light absorption coefficient of the atmospheric aerosol. Atmos. Environ. 29, 875–883.

Houyoux, M.R., Vukovich, J.M., Coats, C.J., Wheeler, N.J.M., Kasibhatla, P.S., 2000. Emission inventory development and processing for the seasonal model for regional air quality (SMRAQ) project. J. Of Geophys. Res. Atmos. 105, 9079–9090.

Jaffe, D.A., Wigder, N., Downey, N., Pfister, G., Boynard, A., Reid, S.B., 2013. Impact of wildfires on ozone exceptional events in the western US. Environ. Sci. Technol. 47, 11065–11072.

Jaffe, D.A., Wigder, N.L., 2012. Ozone production from wildfires: a critical review. Atmos. Environ. 51, 1–10.

Jiang, X., Wiedinmyer, C., Carlton, A.G., 2012. Aerosols from fires: an examination of the effects on ozone photochemistry in the Western United States. Environ. Sci. Technol. 46, 11878–11886.

Jimenez, J., Canagaratna, M., Donahue, N., Prevot, A., Zhang, Q., Kroll, J., DeCarlo, P., Allan, J., Coe, H., Ng, N., 2009. Evolution of organic aerosols in the atmosphere. Science 326, 1525–1529.

Kansas Department of Health and Environment, 2010. State of Kansas Flint Hills Smoke Management Plan December, 2010. http://www.ksfire.org/docs/about/Flint_Hills_SMP_v10FINAL.pdf.

Keywood, M., Kanakidou, M., Stohl, A., Dentener, F., Grassi, G., Meyer, C., Torseth, K., Edwards, D., Thompson, A.M., Lohmann, U., 2013. Fire in the air: biomass burning impacts in a changing climate. Crit. Rev. Environ. Sci. Technol. 43, 40–83.

Kim, Y.H., Tong, H., Daniels, M., Boykin, E., Krantz, Q.T., McGee, J., Hays, M., Kovalcik, K., Dye, J.A., Gilmour, M.I., 2014. Cardiopulmonary toxicity of peat wildfire particulate matter and the predictive utility of precision cut lung slices. Part Fibre Toxicol. 11, 29.

Kleinman, L.I., 1991. Seasonal dependence of boundary layer peroxide concentration: the low and high NO x regimes. J. Geophys. Res. Atmos. 96, 20721–20733.

Kleinman, L.I., 1994. Low and high NOx tropospheric photochemistry. J. Geophys. Res. Atmos. 99, 16831–16838.

Konovalov, I., Beekmann, M., Berezin, E., Petetin, H., Mielonen, T., Kuznetsova, I., Andreae, M., 2015. The role of semi-volatile organic compounds in the meso-scale evolution of biomass burning aerosol: a modelling case study of the 2010 mega-fire event in Russia. Atmos. Chem. Phys. Discuss. 15, 9107–9172.

Koo, B., Knipping, E., Yarwood, G., 2014. An improved volatility basis set for modeling organic aerosol in both CAMx and CMAQ. In: Air Pollution Modeling and Its Application XXIII. Springer, pp. 103–108.

Kwok, R., Baker, K., Napelenok, S., Tonnesen, G., 2015. Photochemical grid model implementation of VOC, NO x, and O 3 source apportionment. Geosci. Model Dev. 8, 99–114.

Kwok, R., Napelenok, S., Baker, K., 2013. Implementation and evaluation of PM2.5 source contribution analysis in a photochemical model. Atmos. Environ. 80, 398–407.

Laskin, A., Laskin, J., Nizkorodov, S.A., 2015. Chemistry of atmospheric brown carbon. Chem. Rev. 115, 4335–4382.

May, A., Lee, T., McMeeking, G., Akagi, S., Sullivan, A., Urbanski, S., Yokelson, R., Kreidenweis, S., 2015. Observations and analysis of organic aerosol evolution in some prescribed fire smoke plumes. Atmos. Chem. Phys. 15, 6323–6335.

May, A.A., Levin, E.J., Hennigan, C.J., Riipinen, I., Lee, T., Collett, J.L., Jimenez, J.L., Kreidenweis, S.M., Robinson, A.L., 2013. Gas-particle partitioning of primary organic aerosol emissions: 3. Biomass burning. J. Geophys. Res. Atmos. 118, 11,327–311,338.

McKeen, S., Wotawa, G., Parrish, D., Holloway, J., Buhr, M., Hübler, G., Fehsenfeld, F., Meagher, J., 2002. Ozone production from Canadian wildfires during June and july of 1995. J. Geophys. Res. Atmos. 107.

National Interagency Fire Center, 2016. Total Wildland Fires and Acres (1960-2015). http://www.nifc.gov/fireInfo/fireInfo_stats_totalFires.html.

National Oceanic and Atmospheric Administration, 2016. NOAA Hazard Mapping System (HMS) Data. http://www.ssd.noaa.gov/PS/FIRE/hms.html.

Nolte, C., Appel, K., Kelly, J., Bhave, P., Fahey, K., Collett Jr., J., Zhang, L., Young, J., 2015. Evaluation of the Community Multiscale Air Quality (CMAQ) model v5. 0 against size-resolved measurements of inorganic particle composition across sites in North America. Geosci. Model Dev. 8, 2877–2892.

Ortega, A., Day, D., Cubison, M., Brune, W., Bon, D., de Gouw, J., Jimenez, J., 2013. Secondary organic aerosol formation and primary organic aerosol oxidation from biomass-burning smoke in a flow reactor during FLAME-3. Atmos. Chem. Phys. 13, 11551–11571.

Paugam, R., Wooster, M., Freitas, S., Val Martin, M., 2015. A review of approaches to estimate wildfire plume injection height within large scale atmospheric chemical transport models–Part 1. Atmos. Chem. Phys. Discuss. 15, 9767–9813.

Pfister, G., Wiedinmyer, C., Emmons, L., 2008. Impacts of the fall 2007 California wildfires on surface ozone: integrating local observations with global model simulations. Geophys. Res. Lett. 35.

Pratt, K., Murphy, S., Subramanian, R., DeMott, P., Kok, G., Campos, T., Rogers, D., Prenni, A., Heymsfield, A., Seinfeld, J., 2011. Flight-based chemical characterization of biomass burning aerosols within two prescribed burn smoke plumes. Atmos. Chem. Phys. 11, 12549–12565.

Pye, H.O., Seinfeld, J.H., 2010. A global perspective on aerosol from low-volatility organic compounds. Atmos. Chem. Phys. 10, 4377–4401.

Raffuse, S., Du, Y., Larkin, N., Lahm, P., 2012. Development of the 2008 wildland fire national emissions inventory. In: 20th International Emissions Inventory Conference, August, pp. 13–16.

Rappold, A.G., Stone, S.L., Cascio, W.E., Neas, L.M., Kilaru, V.J., Sue Carraway, M., Szykman, J.J., Ising, A., Cleve, W.E., Meredith, J.T., 2011. Peat bog wildfire smoke exposure in rural North Carolina is associated with cardiopulmonary emergency department visits assessed through syndromic surveillance. Environ. health Perspect. 119, 1415.

Real, E., Law, K., Weinzierl, B., Fiebig, M., Petzold, A., Wild, O., Methven, J., Arnold, S., Stohl, A., Huntrieser, H., 2007. Processes influencing ozone levels in Alaskan forest fire plumes during long-range transport over the North Atlantic. J. Geophys. Res. Atmos. 112.

Robinson, A.L., Donahue, N.M., Shrivastava, M.K., Weitkamp, E.A., Sage, A.M., Grieshop, A.P., Lane, T.E., Pierce, J.R., Pandis, S.N., 2007. Rethinking organic aerosols: semivolatile emissions and photochemical aging. Science 315, 1259–1262.

Saide, P.E., Peterson, D.A., Silva, A., Anderson, B., Ziemba, L.D., Diskin, G., Sachse, G., Hair, J., Butler, C., Fenn, M., 2015. Revealing important nocturnal and day-to-day variations in fire smoke emissions through a multiplatform inversion. Geophys. Res. Lett. 42, 3609–3618.

Sarwar, G., Appel, K.W., Carlton, A.G., Mathur, R., Schere, K., Zhang, R., Majeed, M.A., 2011. Impact of a new condensed toluene mechanism on air quality model predictions in the US. Geosci. Model Dev. 4, 183–193.

Sarwar, G., Fahey, K., Kwok, R., Gilliam, R.C., Roselle, S.J., Mathur, R., Xue, J., Yu, J., Carter, W.P.L., 2013. Potential impacts of two SO2 oxidation pathways on regional sulfate concentrations: aqueous-phase oxidation by NO2 and gas-phase oxidation by Stabilized Criegee Intermediates. Atmos. Environ. 68, 186–197.

Sillman, S., 1995. The use of NO y, H2O2, and HNO3 as indicators for ozone-NO x-hydrocarbon sensitivity in urban locations. J. Geophys. Res. Atmos. 100, 14175–14188.

Sillman, S., Logan, J.A., Wofsy, S.C., 1990. The sensitivity of ozone to nitrogen oxides and hydrocarbons in regional ozone episodes. J. Geophys. Res. Atmos. 95, 1837–1851.

Simon, H., Baker, K.R., Phillips, S., 2012. Compilation and interpretation of photochemical model performance statistics published between 2006 and 2012. Atmos. Environ. 61, 124–139.

Simon, H., Bhave, P.V., 2012. Simulating the degree of oxidation in atmospheric organic particles. Environ. Sci. Technol. 46, 331–339.

Skamarock, W.C., Klemp, J.B., Dudhia, J., Gill, D.O., Barker, D.M., Duda, M.G., Huang, X., Wang, W., Powers, J.G., 2008. A Description of the Advanced Research WRF Version 3. NCAR Technical Note NCAR/TN-475+STR.

Strand, T., Gullett, B., Urbanski, S., O'Neill, S., Potter, B., Aurell, J., Holder, A., Larking, N., Moore, M., Rorig, M., 2015. Smoke and emissions measurements—RxCADRE 2012 (submitted). J. Wildland Fire 1331–1338.

Tonnesen, G.S., Dennis, R.L., 2000. Analysis of radical propagation efficiency to assess ozone sensitivity to hydrocarbons and NO x: 1. Local indicators of instantaneous odd oxygen production sensitivity. J. Geophys. Res. Atmos. 105, 9213–9225.

Toon, O.B., McKay, C.P., Ackerman, T.P., Santhanam, K., 1989. Rapid calculation of radiative heating rates and photodissociation rates in inhomogeneous multiple scattering atmospheres. J. Geophys. Res. 94, 16287–16301.

U.S. Department of Agriculture, 2011. Wallow Fire 2011 Large Scale Event Recovery Rapid Assessment Team Fire/Fuels Report Apache-Sitgreaves National Forests. http://www.fs.usda.gov/Internet/FSE_DOCUMENTS/stelprdb5333354.pdf.

U.S. Environmental Protection Agency, 2014a. National Emissions Inventory, Version 1 Technical Support Document, 2011. http://www.epa.gov/ttn/chief/net/2011nei/2011_nei_tsdv1_draft2_june2014.pdf.

U.S. Environmental Protection Agency, 2014b. Meteorological Model Performance for Annual 2011 WRF v3.4 Simulation. http://www.epa.gov/ttn/scram/reports/MET_TSD_2011_final_11-26-14.pdf.

U.S. Environmental Protection Agency, 2015. SMOKE v3.7 User's Manual. https://www.cmascenter.org/smoke/documentation/3.7/html/.

Vakkari, V., Kerminen, V.M., Beukes, J.P., Tiitta, P., Zyl, P.G., Josipovic, M., Venter, A.D., Jaars, K., Worsnop, D.R., Kulmala, M., Laakso, L., 2014. Rapid changes in biomass burning aerosols by atmospheric oxidation. Geophys. Res. Lett. 41, 2644–2651.

Wang, Z.S., Chien, C.J., Tonnesen, G.S., 2009. Development of a tagged species source apportionment algorithm to characterize three-dimensional transport and transformation of precursors and secondary pollutants. J. Geophys. Res. Atmos. 114.

Wiedinmyer, C., Akagi, S., Yokelson, R.J., Emmons, L., Al-Saadi, J., Orlando, J., Soja, A., 2011. The Fire INventory from NCAR (FINN): a high resolution global model to estimate the emissions from open burning. Geosci. Model Dev. 4, 625.

Wild, O., Zhu, X., Prather, M.J., 2000. Fast-J: accurate simulation of in-and below-cloud photolysis in tropospheric chemical models. J. Atmos. Chem. 37, 245–282.

Woody, M., Baker, K., Hayes, P., Jimenez, J., Koo, B., Pye, H., 2016. Understanding sources of organic aerosol during CalNex-2010 using the CMAQ-VBS. Atmos. Chem. Phys. 16, 4081–4100.

Zhou, W., Cohan, D.S., Pinder, R.W., Neuman, J.A., Holloway, J.S., Peischl, J., Ryerson, T.B., Nowak, J.B., Flocke, F., Zheng, W.G., 2012. Observation and modeling of the evolution of Texas power plant plumes. Atmos. Chem. Phys. 12, 455–468.